Performance of list mode data acquisition with ECAT EXACT HR and ECAT EXACT HR+ positron emission scanners

Hiroshi Watabe,* Keiichi Matsumoto,** Michio Senda** and Hidehiro Iida*

*Department of Investigative Radiology, National Cardiovascular Center Research Institute
**Institute of Biomedical Research and Innovation

Recently, list mode (event-by-event) data acquisition with positron emission tomography (PET) has been widely noticed because list mode acquisition is superior to conventional frame mode data acquisition in terms of (1) higher efficiency of data storage, (2) higher temporal resolution, and (3) higher flexibility of data manipulation. The aim of this study is to investigate the performance of list mode data acquisition with ECAT EXACT HR and HR+ PET scanners (CTI PET Systems) and its feasibility in clinical applications. A cylindrical phantom (16 cm in diameter and length) filled with a ^{11}C solution for the HR and a ^{15}O solution for the HR+ was scanned several times by varying the radioactivity concentration with the list mode and frame mode acquisitions. The scans were also carried out with a septa (2D mode) and without a septa (3D mode) in order to evaluate the effect of the interplane septa on the quality of the list mode data. The acquired list mode data were sorted into a sinogram and reconstructed using a filtered back-projection algorithm. The count rate performance of the list mode data was comparable to that of the frame mode data. However, the list mode acquisition could not be performed when the radioactivity concentration in the field-of-view was high (exceeding 24 kBq/ml for the 3D mode) due to a lack of sufficient transfer speed for sending data from the memory to hard disk. In order to estimate the pixel noise in a reconstructed image, ten replicated data sets were generated from one list mode data. The reconstructed images with the 3D mode had a signal-to-noise ratio that was more than 60% better than that of the image with the 2D mode. The file size of the generated list mode data was also evaluated. In the case of ECAT EXACT HR+ with the 3D list mode, the list mode data with a generated file size of 2.31 Mbytes/s were generated for 37 MBq injections. Our results suggest that careful attention must be paid to the protocol of the list mode data acquisition in order to obtain the highest performance of the PET scanner.

Key words: PET, list mode, frame mode

INTRODUCTION

Recently, list mode (event-by-event) data acquisition with positron emission tomography (PET) has attracted the attention of many investigators from different fields. In the list mode acquisition, every detected event (both prompt and random) including the location of the line of response in the tomograph is recorded. Although list mode acquisition requires more computational power to process data in comparison to conventional frame mode acquisition, it has several advantages such as (1) higher efficiency of data storage, (2) higher temporal resolution and (3) higher flexibility of data manipulation (flexible frame rebinning, flexible for iterative image reconstruction). Further, many clinical benefits can be expected from the list mode acquisition, for example, real-time motion correction[1,2] and improvement of image quality.[3] However, as compared to the conventional frame mode acquisition, several considerations such as reliability and compatibility must be taken into account before applying

the list mode acquisition for daily clinical routines.

ECAT EXACT HR[4] and ECAT EXACT HR+[5] (CTI/ Siemens, Knoxville, TN, USA) are commercially available PET scanners, which are designed for high spatial resolution, and are employed for research as well as clinical purposes. The goal of this study is to evaluate the performance of the list mode acquisition with ECAT EXACT HR and HR+ scanners and investigate the feasibility of the list mode acquisition in clinical applications. We performed a series of scans of a phantom with the list and frame modes. In order to evaluate the effect of interplane septa on the quality of the list mode data, the scans were carried out with a septa (2D mode) and without a septa (3D mode). The performance of the list mode data acquisition was evaluated with respect to count rate performance, noise property, and generated file size.

MATERIALS AND METHODS

Scanner Description
Table 1 shows the system characteristics of the ECAT EXACT HR scanner in comparison to those of the ECAT EXACT HR+ scanner. Both the scanners have a retractable interplane septa and allow scanning in the 2D mode (with septa) as well as the 3D mode (without septa). For the list mode acquisition, the scanners have a memory of 32 Mbytes for the purpose of gate acquisition. The memory is partitioned into two 16 Mbytes buffers that increment, fill, and write to a hard disk alternately.

Phantom Experiments
We performed phantom experiments for the ECAT EXACT HR scanner at the BF Research Institute (Suita, Osaka, Japan) and ECAT EXACT HR+ scanner at the Institute of Biomedical Research and Innovation (Kobe, Hyogo, Japan). Cylindrical phantoms with a diameter and height of 16 cm were employed for the experiments. A radioactive solution was filled in the phantom and a series of scans were performed with the 2D list, 3D list, 2D frame and 3D frame modes (Table 2). For the EXACT HR scanner, a ^{11}C solution was used, and the duration of each scan was 180 s. For the EXACT HR+ scanner, a ^{15}O solution was used, and the duration of each scan was 30 s. The configurations were different because the experiments were carried out in different institutes using their respective isotopes.

Data Analysis
The obtained list mode data were sorted into sinogram data with a system default span and a maximum ring difference for each scanner (Table 1). The image of each scan was reconstructed using a filtered back-projection technique with a 6-mm Gaussian filter. For the 3D data set, FORE (Fourier rebinning)[6] was applied prior to the reconstruction. The matrix sizes of the reconstructed image were $128 \times 128 \times 47$ for the ECAT EXACT HR

Table 1 System characteristics of ECAT EXACT HR in comparison with those of ECAT EXACT HR+ scanners

	HR	HR+
detector ring (slice)	24 (47)	32 (63)
crystals/ring	784	576
block detector design	8×7	8×8
crystal size (mm)	$5.9 \times 2.9 \times 30$	$4.39 \times 4.05 \times 30$
axial field-of-view (cm)	15.0	15.5
transaxial field-of-view (cm)	51.4	58.3
element number	336	288
number of angle	392	288
default span (2D)	11	15
default span (3D)	7	9
default maximum ring difference (2D)	5	7
default maximum ring difference (3D)	17	22

Table 2 Summary of the scans performed on the phantom

	HR	HR+
	Radioactivity concentration (kBq/m*l*)	Radioactivity concentration (kBq/m*l*)
2D list mode	85.9	135*
	56.1	71.2
	49.8	39.9
	19.4	22.4
	12.4	11.7
3D list mode	24.5*	32.7*
	23.6	21.2
	15.2	14.1
	10.1	13.8
		11.3
		7.65
		5.23
		4.19
2D frame mode	38.8	121
	36.6	61.0
	8.05	30.9
		15.6
		11.1
3D frame mode	19.0	50.4
	15.0	25.5
		12.9
		6.54
		3.31

Radioactivity in the cylindrical phantom when a scan was initiated is shown. * indicates that data are incomplete due to the lack of transfer speed for sending data to the hard disk.

scanner and $128 \times 128 \times 63$ for the ECAT EXACT HR+ scanner. The voxel sizes of the reconstructed image were $1.6 \times 1.6 \times 3.1$ mm for the ECAT EXACT HR scanner and $1.6 \times 1.6 \times 2.4$ mm for ECAT EXACT HR+ scanner.

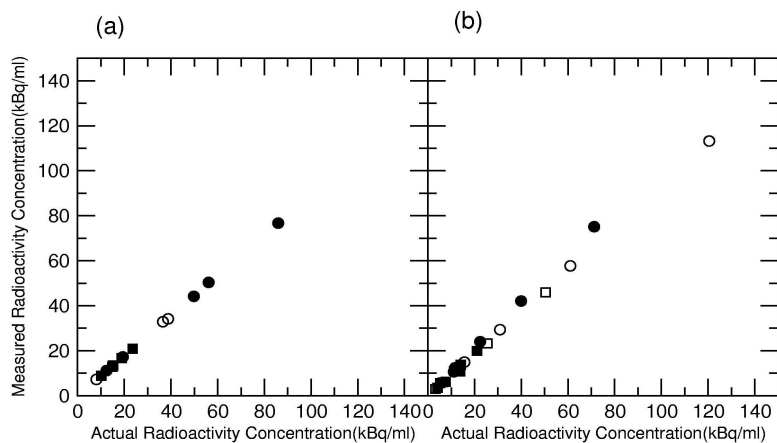Circular ROIs (regions-of-interest) with a diameter of

Fig. 1 Comparison of the actual radioactivity concentration inside the phantom and estimated radioactivity concentration from the reconstructed PET image for the ECAT EXACT HR scanner (a) and ECAT EXACT HR+ scanner (b). The filled circles represent the data from the 2D list mode; filled squares, 3D list mode; open circles, 2D frame mode; and open squares, 3D frame mode.
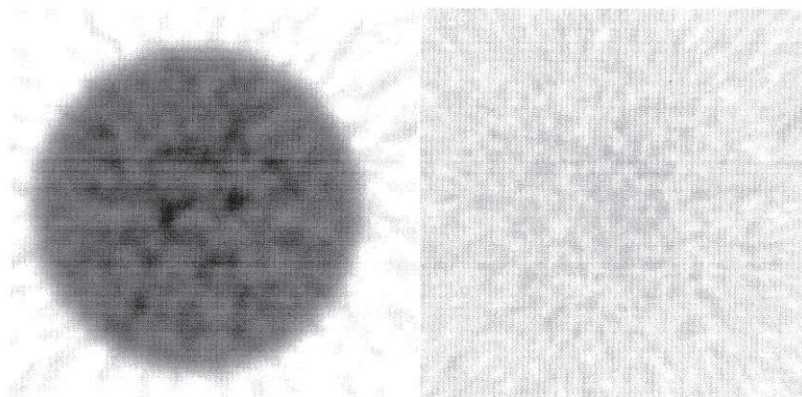

Fig. 2 An example of a generated mean image (*left*) and standard deviation (SD) image (*right*) from 10 replicated data sets generated from one list mode data.
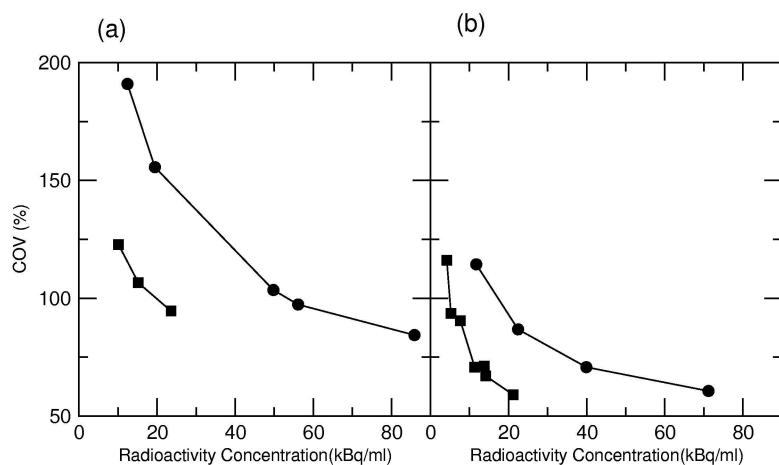

Fig. 3 Relationship between the radioactivity concentration (kBq/m*l*) and mean coefficient of variance (COV) (%) of the pixel count in the reconstructed image for the ECAT EXACT HR scanner (a) and ECAT EXACT HR+ scanner (b). The lines with filled circles represent the data from the 2D list mode and lines with filled squares represent the data from the 3D list mode.
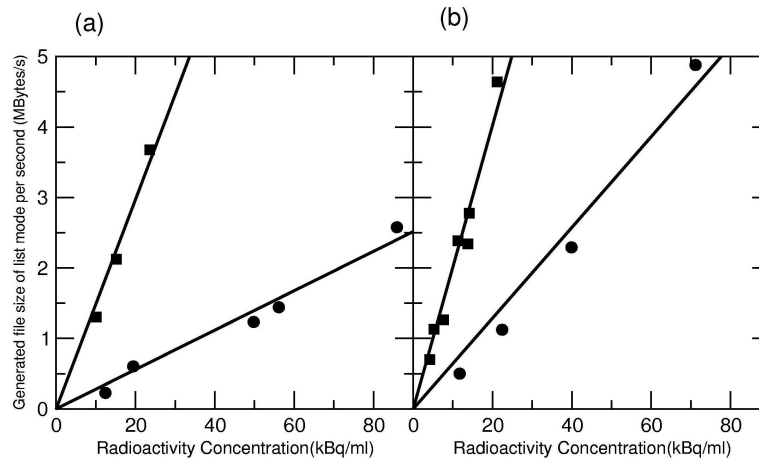
Fig. 4 Relationship between radioactivity concentration (kBq/m*l*) and list mode file size (Mbytes/s) for the ECAT EXACT HR scanner (a) and ECAT EXACT HR+ scanner (b). The filled circles represent the data from the 2D list mode and filled squares represent the data from the 3D list mode. The fitted lines of regression for the data are also shown.

Table 3 Radioactivity concentration in the phantom, NECR (noise equivalent count rate) and COV (coefficient of variance) of the reconstructed image, and the generated list mode file size for the ECAT EXACT HR scanner

Radioactivity concentration (kBq/m*l*)	NECR (/s)	COV (%)	Generated file size per second (Mbytes/s)
	2D list mode		
85.9	9.210×10^4	84.37	2.578
56.1	7.106×10^4	97.32	1.443
49.8	6.423×10^4	103.5	1.234
19.4	4.526×10^4	155.7	0.6034
12.4	1.924×10^4	191.0	0.2279
	3D list mode		
23.6	1.971×10^5	94.57	3.675
15.2	1.465×10^5	106.6	2.123
10.1	1.139×10^5	122.8	1.304

Table 4 Radioactivity concentration in the phantom, NECR and COV of the reconstructed image, and the generated list mode file size for the ECAT EXACT HR+ scanner

Radioactivity concentration (kBq/m*l*)	NECR (/s)	COV(%)	Generated file size per second (Mbytes/s)
	2D list mode		
71.2	1.172×10^5	60.61	4.881
39.9	8.341×10^4	70.73	2.292
22.4	5.470×10^4	86.79	1.124
11.7	3.371×10^4	114.4	0.5012
	3D list mode		
21.2	2.934×10^5	59.05	4.638
14.1	2.331×10^5	67.00	2.779
13.8	1.911×10^5	71.16	2.341
11.3	1.933×10^5	70.76	2.385
7.65	1.214×10^5	90.47	1.263
5.23	1.140×10^5	93.62	1.131
4.19	7.689×10^4	116.1	0.7026

16 cm were placed on the reconstructed image, and the average radioactivity concentration (kBq/m*l*) in the phantom was obtained for each scan.

The NECR (noise equivalent count rate) for each list mode datum was calculated by taking into account the true coincident count rate, random coincident count rate, and scatter fraction in the list mode data.

In order to estimate the noise in a pixel of the reconstructed PET image, 10 replicated data sets were generated from one list mode data. In order to achieve this, the sorting software was modified to produce statistically equivalent multiple sinogram data by splitting the list mode data into pieces. The mean and standard deviation (sd) images were computed from ten reconstructed images. The circular ROIs were placed on both the mean and

sd images, and the averaged mean value ($\bar{m}$) and the averaged sd value ($\bar{s}$) were computed. The average COV (coefficient of variance) for each scan was computed from $\bar{m}$ and $\bar{s}$ by considering the physical decay of a radioisotope as follows:

$$ \text{COV} = \frac{\bar{s}}{\bar{m}} \sqrt{\frac{\lambda}{1 - \exp(-\lambda T)}} \times 100 \ (\%) \qquad (1) $$

where λ is the physical decay constant (s^{-1}) (0.00567 for ^{15}O and 0.000567 for ^{11}C), and T is the scan duration.

The generated file size of the list mode data per second, S (Mbytes/s), was computed for each list mode scan by considering the physical decay of a radioisotope as follows:

$$S = \frac{F\lambda}{1 - \exp(-\lambda T)} \qquad (2)$$

where F (Mbytes) is the generated file size of the list mode data.

RESULTS

Figure 1 (a and b) shows the comparison between the actual radioactivity concentration inside the phantom and the estimated radioactivity concentration from the reconstructed PET image for the ECAT EXACT HR and ECAT EXACT HR+ scanners, respectively. As shown in these figures, there is a good agreement between the list mode data and frame mode data. However, as mentioned in Table 2, if the radioactivity in the field-of-view of the scanner is large, the acquisition of the list mode data would fail due to a lack of sufficient transfer speed for sending data to the hard disk.

Figure 2 shows an example of the generated mean and sd images from the list mode data set. Tables 3 and 4 list the summarized results of the radioactivity concentration in the phantom, NECR and COV in the image, and generated file size of the list mode data for the ECAT EXACT HR and ECAT EXACT HR+ scanners, respectively. Figure 3 shows the relationship between the radioactivity concentration in the phantom and COV in the reconstructed image. As shown in this figure, the image with the 3D acquisition mode has a signal-to-noise ratio that is more than 60% better than that of the image with the 2D acquisition mode. Figure 4 shows the relationship between the radioactivity in the phantom and generated file size of the list mode data. We fitted a line of regression between the radioactivity concentration (A (kBq/ml)) and generated file size (S (Mbytes/s)), and the fitted results are as follows:

$S = 2.79 \times 10^{-2} \times A$ for 2D list mode and ECAT EXACT HR
$S = 1.49 \times 10^{-1} \times A$ for 3D list mode and ECAT EXACT HR
$S = 6.43 \times 10^{-2} \times A$ for 2D list mode and ECAT EXACT HR+
$S = 2.01 \times 10^{-1} \times A$ for 3D list mode and ECAT EXACT HR+
$$(3)$$

DISCUSSION

Although the list mode acquisition is not a new technique, the techniques related to the list mode acquisition[3,7–9] have recently become popular due to their advantage as powerful computing systems. Besides the several favorable features of list mode data, additional consideration is required if the list mode acquisition is to be routinely carried out in clinical applications.

Tables 3 and 4 list useful information for scheduling a PET scan with the list mode acquisition. For instance, the injected activity for a patient must be carefully determined by considering 1) the upper limitation of radioac-

tivity concentration, 2) noise in the image and 3) generated file size. The more photons are detected, the larger list mode data are generated. Therefore, generated file size is important from the practical point of view, such as limited size of data storage, time consuming data processes and data backup. According to Eq. (3), assuming that the radioactivity concentration in the field-of-view of the scanner is 10 kBq/ml, a study of ^{15}O for 2 min generates 24.3 Mbytes, 130 Mbytes, 56.0 Mbytes, and 175 Mbytes for the HR 2D list mode, HR 3D list mode, HR+ 2D list mode, and HR+ 3D list mode, respectively. In the case of a ^{11}C study for one hour, 428 Mbytes, 2.29 Gbytes, 987 Mbytes, and 3.01 Gbytes of the list mode data are generated for the HR 2D list mode, HR 3D list mode, HR+ 2D list mode, and HR+ 3D list mode, respectively. In the case of ^{18}F study for one hour, 836 Mbytes, 4.46 Gbytes, 1.93 Gbytes and 6.02 Gbytes for HR 2D list mode, HR 3D list mode, HR+ 2D list mode, HR+ 3D list mode, respectively. The file size of the list mode data for the ECAT EXACT HR+ scanner is larger than that for the ECAT EXACT HR scanner and interestingly the file size of the frame mode for ECAT EXACT HR scanner is larger than that for ECAT EXACT HR+ scanner (sizes of the single-frame sinogram data are 6.2 Mbytes, 23.1 Mbytes, 5.2 Mbytes and 19.8 Mbytes for the HR 2D frame mode, HR 3D frame mode, HR+ 2D frame mode, and HR+ 3D frame mode, respectively).

As shown in Figure 3, the pixel noise in the reconstructed image can be estimated from the list mode data; this is one of the advantages of list mode acquisition. Using multiple frames with very short time duration, the pixel noise can be obtained by the frame mode data. However, it is not ideal due to physical decay of the radioisotope during data acquisition. The pixel noise obtained from the list mode data is quantitatively comparable among scanners. This figure suggests that the noise property of the ECAT EXACT HR+ scanner is superior to that of the ECAT EXACT HR scanner. This is due to the ECAT EXACT HR+ scanner having a higher sensitivity than ECAT EXACT HR scanner, although the two scanners have different system configurations (Table 1). Further, the comparison of the two scanners is complicated.

As shown in Figure 1, the count rate performance of the frame mode and list mode are not surprisingly in good agreement with each other. However, a difference might be observed between the two data sets because of the higher temporal resolution of the list mode data; this enables the accurate correction of the dead-time of the detector and physical decay of the radioisotope. We used the ACS-II (an advanced computational system that is dedicated to handle data from the PET scanner) for both ECAT EXACT HR and HR+ scanners, and the maximum speed of data transfer from the memory to hard disk appears to be approximately 6 Mbytes/s. A read/write controller on the ACS-II with a memory of 32 Mbytes is split into two buffers of approximately 16 Mbytes each.

When the list mode data is being stored from buffer 1 to the hard disk, data are simultaneously written to buffer 2. Once buffer 2 is filled, data are then written to buffer 1, and the data in buffer 2 are written to the hard disk. Since the speed of our hard disk is 6 Mbytes/s and a single event of the list mode data comprises 4 bytes, 1.5 M events/s can be handled. On the other hand, it takes 2.6 s to clear the 16 Mbyte memory. Therefore, if the occurrence of events exceeds 1.5 M events/s, the ACS-II cannot handle all the events.

For usual clinical PET studies, the existence of more than 74 MBq of radioactivity (i.e. 23 kBq/m*l* assuming cylinder with 16 cm diameter) in the field-of-view is not frequent. However, not only true events but also random events are stored in the list mode data and the radioactivity outside the field-of-view must also be considered. It should be noted that since all the possible line of responses are recorded in the list mode data, the number of prompt and random events in the list mode data are greater than those in the frame mode data.

Phantom experiments are often performed with NECR plotted against activity concentration in order to determine the maximum performance of the scanner in terms of image quality. The radioactivity concentrations of about 80 kBq/m*l* and 20 kBq/m*l* give the highest NECR in 2D mode and 3D mode for the ECAT EXACT HR scanner, respectively.[4] These numbers are interestingly close to the maximum radioactivity concentration for the list mode acquisition in our experiments (see Table 2). This suggests the image quality with the list mode can be comparable with that with the frame mode.

In order to use the list mode acquisition at a clinical site, it is also important that a PET scanner be capable of promptly showing the reconstructed PET images. Before reconstruction, a sorting process is necessary for the list mode data, which results in a longer reconstruction time than that for the conventional frame mode data (It takes 0.2 s per 1 M byte of the list mode data for sorting using PC with Xeon CPU (2.4 GHz) and 1 G byte physical memory). Because each event in the list mode data is sequentially stored, it is easy to implement a parallel sorting process. In order to accelerate data processing, the sorting of the list mode data can be performed on a PC cluster[10] which is currently available at a low cost.

The list mode acquisition has several advantages over the conventional frame mode acquisition as mentioned in the first section. However, two disadvantages of the list mode acquisition addressed in this paper, namely, upper limitation of radioactivity and large file size, obstruct the applications of the list mode data on a daily basis. These disadvantages will be overcome along with advances in hardware and software.

CONCLUSION

A series of phantom studies revealed the physical characteristics of the list mode data acquisition with ECAT EXACT HR and HR+ scanners. This study suggests that careful attention must be paid to the protocol of the list mode data acquisition in order to obtain the highest performance of the PET scanner in clinical applications.

ACKNOWLEDGMENT

REFERENCES

1. Bloomfield PM, Spinks TJ, Reed J, Schnorr L, Westrip AM, Livieratos L, et al. The design and implementation of a motion correction scheme for neurological PET. *Phys Med Biol* 2003; 48 (8): 959–978.
2. Woo SK, Watabe H, Choi Y, Kim KM, Park CC, Bloomfield PM, et al. Sinogram-based motion correction of PET images using optical motion tracking system and list-mode data acquisition. *IEEE Trans Nucl Sci* 2004; 51 (3): 782–788.
3. Nichols TE, Qi J, Asma E, Leahy RM. Spatiotemporal reconstruction of list-mode PET data. *IEEE Trans Med Imaging* 2002; 21 (4): 396–404.
4. Wienhard K, Dahlbom M, Eriksson L, Michel C, Bruckbauer T, Pietrzyk U, et al. The ECAT EXACT HR: Performance of a new high resolution positron scanner. *J Comput Assist Tomogr* 1994; 18 (1): 110–118.
5. Brix G, Zaers J, Adam LE, Bellemann ME, Ostertag H, Trojan H, et al. Performance evaluation of a whole-body PET scanner using the NEMA protocol national electrical manufacturers association. *J Nucl Med* 1997; 38 (10): 1614–1623.
6. Defrise M, Liu X. A fast rebinning algorithm for 3D positron emission tomography using Johns equation. *Inverse Problems* 1999; 15: 1047–1065.
7. Huesman RH, Klein GJ, Moses WW, Qi J, Reutter BW, Virador PR. List-mode maximum-likelihood reconstruction applied to positron emission mammography (PEM) with irregular sampling. *IEEE Trans Med Imaging* 2000; 19 (5): 532–537.
8. Levkovitz R, Falikman D, Zibulevsky M, Ben-tal A, Nemirovski A. The design and implementation of cosem, an iterative algorithm for fully 3-D listmode data. *IEEE Trans Med Imaging* 2001; 20 (7): 633–642.
9. Byrne C. Likelihood maximization for list-mode emission tomographic image reconstruction. *IEEE Trans Med Imaging* 2001; 20 (10): 1084–1092.
10. Watabe H, Woo Sk, Kim KM, Kudomi N, Iida H. Performance improvement of event-based motion correction for PET using a PC cluster. Conference Record of IEEE Trans Nuclear Science and Medical Imaging Coeference, 2003.